Mitochondrion 25 (2015) 104–112

Contents lists available at ScienceDirect

Mitochondrion

journal homepage: www.elsevier.com/locate/mito

Differences in mitochondrial function in homogenated samples from healthy and epileptic specific brain tissues revealed by high-resolution respirometry

Johannes Burtscher [a], Luca Zangrandi [a], Christoph Schwarzer [a,*], Erich Gnaiger [b,c,**]

[a] Dept. Pharmacology, Medical University Innsbruck, Peter-Mayr-Str. 1a, 6020 Innsbruck, Austria
[b] D. Swarovski Research Laboratory, Department of Visceral, Transplant and Thoracic Surgery, Medical University Innsbruck, Anichstr. 35, 6020 Innsbruck, Austria
[c] OROBOROS INSTRUMENTS, Schöpfstr. 18, 6020 Innsbruck, Austria

ARTICLE INFO

Article history:
Received 10 March 2015
Received in revised form 20 October 2015
Accepted 23 October 2015
Available online 26 October 2015

Keywords:
Neurodegeneration
Epilepsy
Mitochondria
Brain regions
Respirometry

ABSTRACT

Mitochondrial dysfunction and oxidative stress are strongly implicated in neurodegenerative diseases and epilepsy. Strikingly, neurodegenerative diseases show regional specificity in vulnerability and follow distinct patterns of neuronal loss. A challenge is to understand, why mitochondria fail in particular brain regions under specific pathological conditions. A potential explanation could be provided by regional or cellular specificity of mitochondrial function.

We applied high-resolution respirometry to analyze the integrated Complex I- and II (CI and CII)-linked respiration, the activity of Complex IV, and the combined CI&II-linked oxidative phosphorylation (OXPHOS)- and electron-transfer system (ETS)-capacity in microsamples obtained from distinct regions of the mouse brain. We compared different approaches to assess mitochondrial density and suggest flux control ratios as a valid method to normalize respiration to mitochondrial density.

This approach revealed significant differences of CI- and CII-linked OXPHOS capacity and coupling control between motor cortex, striatum, hippocampus and pons of naïve mice. CI-linked respiration was highest in motor cortex, while CII-linked respiration predominated in the striatum. To investigate if this method could also determine differences in normal and disease states within the same brain region, we compared hippocampal homogenates in a chronic epilepsy model. Three weeks after stereotaxic injection of kainate, there was a down-regulation of CI- and upregulation of CII-linked respiration in the resulting epileptic ipsilateral hippocampus compared to the contralateral one.

In summary, respirometric OXPHOS analysis provides a very sensitive diagnostic approach using small amounts of distinct brain tissues. In a single assay, information is obtained on numerous OXPHOS parameters as indicators of tissue-specific mitochondrial performance.

© 2015 The Authors. Elsevier B.V. and Mitochondria Research Society. This is an open access article under the CC BY-NC-ND license (http://creativecommons.org/licenses/by-nc-nd/4.0/).

1. Introduction

The most prevalent neurodegenerative diseases share common pathophysiological mechanisms, such as mitochondrial dysfunction, oxidative stress, and cell death, yet the particular neuronal population involved dictates the symptomatic presentation of disease. Parkinson's disease and Huntington's disease, but also familial amyotrophic lateral sclerosis, Alzheimer's disease and some types of epilepsies are characterized by severe neuronal losses. Strikingly, neuronal losses show high regional specificity and frequently follow distinct patterns: Parkinson's disease affects mainly dopaminergic neurons in the substantia nigra (Hirsch et al., 1988), while Huntington's disease is associated with neuronal loss in the motor cortex and striatum (Lange et al., 1976). One research focus in our quest to understand this phenomenon is mitochondrial dysfunction and oxidative stress. Mitochondrial dysfunction may be restricted to affected regions and heterogeneity of mitochondrial parameters has been described in different brain areas (for review see Dubinsky, 2009). However, a major unanswered question is if region-specific differences in basal mitochondrial function predispose select neuronal populations to pathological stimuli, or if mitochondrial energetics are similar throughout, but the neurons are selectively vulnerable to events downstream of mitochondrial dysfunction.

* Corresponding author.
** Correspondence to: E. Gnaiger, Daniel Swarovski Research Laboratory, Department of Visceral, Transplant and Thoracic Surgery, Medical University Innsbruck, Anichstr. 35, 6020 Innsbruck, Austria.
E-mail addresses: Schwarzer.Christoph@i-med.ac.at (C. Schwarzer), Erich.Gnaiger@i-med.ac.at (E. Gnaiger).

http://dx.doi.org/10.1016/j.mito.2015.10.007
1567-7249/© 2015 The Authors. Elsevier B.V. and Mitochondria Research Society. This is an open access article under the CC BY-NC-ND license (http://creativecommons.org/licenses/by-nc-nd/4.0/).

Oxidative phosphorylation (OXPHOS) is a major player in energy transformation, where the subsystems of the electron transfer system (ETS) generate the transmembrane protonmotive force and the phosphorylation system utilizes the protonmotive force. The main ETS protein complexes are located in the inner mitochondrial membrane and pump protons to drive the phosphorylation of ADP to ATP. Dysfunction of a single protein or entire complex of the OXPHOS-machinery due to genetic mutations cannot explain per se the regional specificity of neurodegenerative diseases. However, the expression of mitochondrial proteins is regulated epigenetically, therefore regional or even cellular specificity of the contribution of distinct complexes may be regulated by cell specific gene expression mechanisms.

Specifically Complexes I, II and IV (CI, CII and CIV) in distinct brain regions are presently discussed as being affected in a number of classical neurodegenerative diseases, such as Parkinson's disease (Schapira et al., 1989), Huntington's disease (Gu et al., 1996) and Alzheimer's disease (Crouch et al., 2005) as well as in several types of epilepsies (for reviews see (Baron et al., 2007; Waldbaum and Patel, 2010a), such as temporal lobe epilepsy (Kunz et al., 2000). Accordingly, the contribution of the distinct complexes to mitochondrial function needs to be studied in a regionally-specific context in order to reveal the causal relationship between mitochondrial vulnerability and pathological processes. Isolated mitochondria are often used to study mitochondrial parameters in cells or tissues (Perry et al., 2013). By contrast studying distinct mitochondrial functions in brain microsamples requires a method with low preparative loss and close to physiological tissue environments. Recently, Herbst and Holloway (Herbst and Holloway, 2015) compared the respiration of permeabilized brain tissues and mitochondria isolated from cortex. They conclude that permeabilized brain tissue offers several advantages, such as minimization of time and tissue required for measurements carried out under more physiological mitochondrial conditions.

The aim of the present study was to establish a further developed method, which would enable detailed analysis of mitochondrial functional within specific regions of the brain. Considering the ongoing discussions on mitochondrial complexes involved in neurological diseases, the main focus was put on integrated CI-, and CII-linked mitochondrial pathways under coupled and noncoupled conditions, and the single enzymatic step of cytochrome *c* oxidase (CIV; Gnaiger, 2014). A complex substrate-uncoupler-inhibitor-titration (SUIT) protocol was applied for mitochondrial phenotyping (comprehensive OXPHOS analysis) in a single incubation of small tissue samples of 2 mg fresh weight. The method was sufficiently sensitive to reveal functional differences between distinct brain areas in control animals, and between the ipsi- and contralateral dorsal hippocampi in a mouse model of temporal lobe epilepsy. The omission of detergents in the tissue preparation and our SUIT-protocol allow evaluation of several subsequentially targeted substrate and coupling states without compromising the stability of respiration. Reference states addressed within a SUIT protocol can be selected as internal functional mitochondrial markers, which have been validated in this study.

2. Materials and methods

2.1. Animals and tissue preparation

Six male C57Bl/6J mice (http://www.criver.com/products-services/basic-research/find-a-model/jax-mice-strain-c57bl-6j), 15–20 weeks old and 28–30 g on the respective experimental day, were used for experiments of different brain regions. Ten C57Bl/6 N mice (http://www.criver.com/products-services/basic-research/find-a-model/c57bl-6n-mouse), 16–20 weeks old, 27–29 g, were injected with either saline ($N = 6$) or kainic acid ($N = 4$) for experiments on temporal lobe epilepsy. The saline or kainic acid injected mice were sacrificed 2.5–3.5 or 3.0–3.5 weeks, respectively, after injections for respirometric studies. Mice were kept at 23 °C with 12/12 light/dark cycle and free access to standard laboratory rodent chow and water. All procedures involving animals were approved by the Austrian Animal Experimentation Ethics Board in compliance with the European convention for the protection of vertebrate animals used for experimental and other scientific purposes ETS no.: 123. Every effort was taken to minimize the number of animals used.

Cervical dislocation was performed between 9.30 am and 10.30 a.m. immediately before OXPHOS analysis to minimize circadian rhythm effects.

Brains were micro-dissected on ice and specimens weighed on an analytical balance (Mettler Toledo AE 160, Greifensee, Switzerland). The micro-dissected brain regions were directly transferred into ice-cold mitochondrial respiration medium (MiR06Cr in a 12 well plate) containing 280 IU/ml catalase (Pesta and Gnaiger, 2012) and 20 mM creatine.The remaining blood was removed by washing in MiR06Cr. Subsequently tissues were homogenized in the same medium in a pre-cooled glas potter (tight fit; WiseStir homogenizer HS-30E, witeg Labortechnik GmbH, Wertheim, Germany) at 1000 rpm, with 10 strokes for motor cortex and striatum, but 15 strokes for hippocampus and brainstem (pons). Resulting homogenates containing 5 mg tissue wet weight were suspended in 5 ml of ice-cold MiR06Cr and 2×2.1 ml of this suspension were used for OXPHOS-analysis in duplicates. Residual homogenates were frozen at −80 °C for protein quantification and citrate synthase activity determination.

An alternative homogenization method was tested for the experiments on epileptic hippocampal (dorsal hippocampi) tissue. Tissues were weighed, cut and homogenized in a PBI-Shredder (OROBOROS INSTRUMENTS, Innsbruck, Austria) for 10 s in position 1 and 10 s in position 2. For hippocampal tissue, highly comparable homogenate preparations could be achieved also with this method. For comparable homogenization of different tissues, the above-mentioned method for homogenization in a glass potter was superior.

Respiration was higher in potter preparations after 10–15 strokes than after fewer strokes or in first spin homogenates (in which mitochondria in the homogenate were enriched in the supernatant by a centrifugation step of 2000 g for 3 min at 4 °C). Respiratory fluxes for the optimized potter preparations were similar to shreddering.

The optimized potter preparation of brain tissue yields a high degree of permeabilization as evident by the minimal effect of digitonin titrations on OXPHOS capacity. Therefore, digitonin is not necessary for this protocol. The effect of digitonin was more evident in shredder homogenates. Homogenate preparation with 10–15 strokes of the potter resulted consistently in a variance of respiratory flux between duplicates, which was 3-fold lower than in preparations using the PBI shredder.

No cytochrome *c*-effect, indicating outer mitochondrial membrane damage, was observed for any of the tested methods. For this test, 10 μM cytochrome c were applied after addition of substrates for CI and ADP.

We cannot exclude that synaptosomes might have been present in the tissue homogenates.

2.2. Kainic acid injection

Mice were sedated with an ip injection of ketamine (160 mg/kg; Graeub Veterinary Products, Switzerland) and then deeply anesthetized with sevoflurane through a precise vaporizer (Midmark, USA). Mice were injected with 1 nmole kainic acid (20 mM; KA, Ocean Produce International, Canada) solution into CA1 region of the left hippocampus as previously described (Loacker et al., 2007).

2.3. High-resolution respirometry

Tissue homogenates were transferred into calibrated Oxygraph-2 k (O2k, OROBOROS INSTRUMENTS, Innsbruck, Austria) 2 ml-chambers. Oxygen polarography was performed at 37 ± 0.001 °C (electronic

Peltier regulation) in O2k-chambers and oxygen concentration (μM) as well as oxygen flux per tissue mass (pmol $O_2.s^{-1}\cdot mg^{-1}$) were recorded real-time using DatLab software (OROBOROS INSTRUMENTS, Innsbruck, Austria). Injections of 1–3 μl 200 mM H_2O_2 (instantaneously dismutated by catalase in the medium to oxygen and water) were used for oxygenation at the beginning of each experiment until an oxygen concentration of 360–380 μM was reached.

In the present SUIT protocol, non-phosphorylating LEAK-respiration (CI_L) was induced by adding the CI-linked substrates pyruvate (5 mM), malate (0.5 mM) and glutamate (10 mM; Suppl. Fig. 1, step 1). Subsequently, OXPHOS-capacity of CI-linked activity (CI_P) was measured after addition of a saturating concentration of ADP (2.5 mM; Suppl. Fig. 1, step 2). OXPHOS-capacity with combined CI and II-linked substrates ($CI\&II_P$) was assessed by addition of succinate (10 mM; Suppl. Fig. 1, step 3). Stepwise titration of the protonophore carbonyl cyanide m-chloro phenyl hydrazone (CCCP, 0.5 μM steps; Suppl. Fig. 1, step 4) leads to proton leakage through the inner mitochondrial membrane, and was used for the measurement of the capacity of the electron transfer system (ETS, $CI\&II_E$), which is the noncoupled state at optimum uncoupler concentration for maximum oxygen flux. Subsequent inhibition of CI by rotenone (0.5 μM; Suppl. Fig. 1, step 5) provided measurement of CII-linked ETS capacity (CII_E). To control for other oxygen-consuming processes, CII and CIII were inhibited by malonate and antimycin A, respectively (Suppl. Fig. 1, step 6). The resulting residual oxygen consumption (ROX) reflects oxygen consumption from undefined sources and was subtracted from mitochondrial respiratory states (Gnaiger, 2014). ROX was very low, demonstrating the mitochondrial origin of oxygen consumption. In the potter homogenates, ROX was 2.7 ± 0.7%, 3.1 ± 0.2%, 2.9 ± 1.3% and 2.9 ± 0.4% (means ± SD) of the ETS-capacity in brainstem, hippocampus, motor cortex and striatum samples, respectively. For hippocampal shredder homogenates ROX was 5.3 ± 0.4% of the ETS capacity. Oxygen-concentration in the chambers was kept high enough to avoid oxygen limitation of respiration (more than 150 μM O_2 until the end of $CI\&II_P$).

The SUIT protocol was extended for measurement of the single step of CIV activity. The medium was reoxygenized and ascorbate (2 mM) and *N*,*N*,*N*′,*N*′-Tetramethyl-p-phenylenediamine dihydrochloride (TMPD, 0.5 mM) were added. TMPD was maintained in a reduced state by ascorbate and reduces cytochrome *c*. Chemical background oxygen consumption induced by auto-oxidation of TMPD and ascorbate reactions was assessed after inhibition of CIV by sodium azide (100 mM) and reoxygenation with gaseous oxygen (Renner et al., 2002). All reagents used for high-resolution respirometry were purchased from Sigma-Aldrich (St. Louis, Missouri, US).

Respiratory fluxes were corrected automatically for instrumental background by DatLab taking into account oxygen consumption of the oxygen sensor and oxygen diffusion out of or into the oxygraph chamber measured at experimental conditions in incubation medium without biological sample (Gnaiger, 2001). CIV activity was corrected for chemical background oxygen consumption at the specific experimental oxygen concentration.

2.4. Data analysis

Tissue-mass specific oxygen fluxes were compared in different substrate and coupling states after correction for ROX.

Flux control ratios (*FCR*) were calculated by dividing fluxes in all respiratory states of the SUIT protocol (Suppl. Fig. 1) by CI&II-linked ETS-capacity taken as a common reference state (Gnaiger, 2009). In contrast, flux control factors (*FCF*) express the change of flux in a single step of the SUIT protocol, normalized for the high flux as a specific reference state (Gnaiger, 2014). Stimulation of ADP-saturated OXPHOS capacity, *P*, by optimum uncoupler concentration yields ETS capacity, *E*. The stimulatory effect, *E*-*P*, quantifies the limitation of ETS capacity by the capacity of the phosphorylation system. This was determined in the state of maximum ETS capacity supported by CI&II-linked substrates. The corresponding *FCF* is the apparent excess ETS capacity calculated as $(E\text{-}P)/E = 1\text{-}P/E$.

The respiratory acceptor control ratio ($RCR = P/L$) was obtained in the CI-linked substrate state (Suppl. Fig. 1). For statistical analysis RCR was transformed to its respective *FCF*, which is the OXPHOS coupling efficiency calculated as $(P\text{-}L)/P = 1\text{-}L/P$ (Gnaiger, 2014).

The *FCF* for CI-linked substrates stimulating CII-linked respiration was measured as the rotenone effect, 1 – CII/CI&II, in the ETS state in our SUIT protocol. The corresponding *FCF* for the CII-linked substrate (succinate effect) was calculated as 1 – CI/CI&II, determined in the OXPHOS state in the SUIT protocol (Suppl. Fig. 1).

2.5. Protein quantification

The DC™ Protein Assay (Bio-Rad, Hercules, California, US) was used for quantification of protein contents of the homogenized samples. The assay was performed according to the manual, except that the amounts of reagents A and B were reduced by half (250 μl and 2 ml were used, respectively). 100 μl of standards and samples were used and absorbance was read at 750 nm in a spectrophotometer (Hitachi U-2000, Tokyo, Japan). Measurements were performed in duplicates (coefficient of variation between duplicates was 3.4%) and corrected for the absorbance measured in the MiR06Cr medium only.

2.6. Citrate synthase activity

Citrate synthase activity was determined by diluting brain sample homogenates 1:100 in a solution containing 0.25% of Triton X-100 (in a.d.), 0.31 mM Acetyl-CoA (in a.d.), 0.1 mM 5,5′-Dithiobis(2-nitrobenzoic acid) (DTNB) in 1 M Tris(hydroxymethyl)aminomethane-HCl-buffer (pH 8.1) and 0.5 mM oxalacetate in 0.1 M triethanolamine-HCl-buffer (pH 8.0). Absorbance of each sample was measured spectrophotometrically every 10 s across 200 s at 412 nm to detect the absorbing enzyme reaction product TNB (thionitrobenzoic acid) and the rate of absorbance change per min was used to calculate the specific citrate synthase activity *v* (see supplementary method for formula). Samples were measured in duplicates at a tissue concentration of 2 mg/ml.

2.7. Statistical analyses

Results are presented as means ± SEM. One-way ANOVAs were used to compare oxygen fluxes or ratios of the different brain regions in defined states, and Tukey's multiple comparison tests were performed to test differences post hoc. A p-value < 0.05 was considered statistically significant. Variation of marker-values is given in SD in %. Pearson correlations were calculated for mitochondrial marker comparisons separately for the investigated brain regions and for testing differences between *FCF*s for CI- and CII-control of respiration.

3. Results

3.1. Optimization of analytical steps

The present SUIT protocol represents an extension of previous developments (Pesta and Gnaiger, 2012). Due to the inhibitory action of malate on succinate dehydrogenase (CII, unpublished data), we reduced the concentration from 2 mM to 0.5 mM. This did not limit CI-linked OXPHOS capacity in the hippocampus, since an increase from 0.5 to 2 mM malate was without significant effect on CI_P (33.1 ± 4.2 pmol $O_2.s^{-1}\cdot mg^{-1}$ versus 30.9731.0 ± 3.7 pmol $O_2.s^{-1}\cdot mg^{-1}$; $N = 4$). Similarly, the ADP-concentration of 2.5 mM was saturating, since no increase of respiration was observed when ADP was increased from 2 to 3 mM in hippocampus, or from 2.5 mM to 5 mM in hippocampal, striatal or cortical homogenates prepared with the shredder.

The reliability of wet weight measurements was tested by protein quantification of the homogenized samples (Suppl. Fig. 2).

3.2. Assessment of mitochondrial density

Mitochondrial density was similar in all tested brain regions according to consistent results with different mitochondrial markers: citrate synthase (CS) enzyme activity, CIV enzyme activity, and CI&II-linked ETS-capacity CI&II$_E$ (Fig. 1). Variability (SD) of all investigated brain regions pooled were 14.6%, 14.4% and 15.1%, respectively. All functional mitochondrial markers were strongly correlated (CS and CI&II$_E$: $r = 0.80$, $p < 0.001$, CIV and CI&II$_E$: $r = 0.83$, $p < 0.001$, CS and CIV: $r = 0.55$, $p = 0.005$).

Respiratory acceptor control ratios (P/L) for CI-linked respiration were transformed to the flux control factor ($1\text{-}L/P$) for statistical analysis and no differences were found across all tested brain regions ($p = 0.905$, $F_{3/20} = 0.186$, Fig. 2). Apparent ETS excess capacities ($1\text{-}P/E$) in the CI&II-linked substrate state were significantly different between hippocampus and motor cortex ($p = 0.015$, $F_{3/18} = 4.609$; Fig. 2).

3.3. Differences in tissue-mass specific oxygen fluxes across the different brain regions

When comparing tissue-mass specific oxygen fluxes per mg wet weight of brain tissue, we found no differences in the LEAK state, CI$_L$, in which saturating concentrations of CI-linked substrates, but no exogenous ADP was present ($p = 0.414$, $F_{3/20} = 0.998$, Fig. 3A). Upon addition of saturating concentrations of ADP (CI$_P$), the oxygen flux in motor cortex was significantly higher than in all other investigated brain-regions ($p = 0.004$, $F_{3/20} = 5.976$) (Fig. 3B). Addition of succinate to measure CI&II$_P$ resulted in similar oxygen fluxes between all regions again (Fig. 3C) and no difference was also observed after application of uncoupler for assessment of the maximal ETS-capacity ($p = 0.266$, $F_{3/18} = 1.435$, Fig. 1). Subsequent inhibition of CI by rotenone provided CII$_E$, which was highest in the striatum ($p = 0.013$, $F_{3/20} = 4.660$) and significantly lower in the hippocampus (Fig. 3D).

3.4. Differences in flux control ratios across the different brain regions

Comparison of *FCR*s between the different states and brain regions revealed no significant differences across regions in the LEAK-state (CI$_L$) ($p = 0.776$, $F_{3/18} = 0.370$, Fig. 4A). CI$_P$ in the motor cortex was significantly higher ($p < 0.001$, $F_{3/18} = 8.908$) than in all other brain regions (Fig. 4B). CII$_E$ was highest in the striatum ($p = 0.004$, $F_{3/18} = 6.497$) (Fig. 4C) as compared to all other brain regions.

3.5. CI-linked respiration is highest in the motor cortex, CII-linked respiration is highest in the striatum

The CI-linked OXPHOS capacity was higher in motor cortex as compared to other brain tissues (Fig. 5B). CII$_E$ was highest in the striatum (Fig. 5A). The ratio CI/CII is significantly higher in the motor cortex ($p = 0.001$, $F_{3/18} = 7.931$) than in all other investigated brain regions (Fig. 5C).

A negative correlation can be expected theoretically between the CI *FCF* and CII *FCF*, However, the CI *FCF* exhibited a relatively low variability across the investigated brain regions as compared to CII FCF (Suppl. Fig. 3). Whereas the relation between the CI *FCF* and CII *FCF* in hippocampus and brainstem strongly overlap, two clearly separated clusters were observed for motorcortex and striatum. In order to investigate mutual effects of CI *FCF* and CII *FCF*, the correlation was calculated for the data of all brain regions, which was highly significant ($p = 0.003$, Pearson $r = -0.596$).

3.6. Effects on OXPHOS in a mouse model of temporal lope epilepsy

Tissue-mass specific oxygen fluxes were similar in mice injected with saline or with kainic acid (KA) in CI$_L$ ($p = 0.103$, $F_{3/8} = 2.427$, Fig. 6A), CI&II$_P$ (Fig. 6C, $p = 0.115$, $F_{3/8} = 2.316$), CI&II$_E$ (Fig. 6E, $p = 0.098$, $F_{3/8} = 2.482$), and CII$_E$ ($p = 0.424$, $F_{3/8} = 0.987$, Fig. 6E) in the injected (ipsilateral) dorsal hippocampus and in the contralateral dorsal hippocampus. CIV-activity (Fig. 6F, $p = 0.199$, $F_{3/8} = 1.739$) did not differ across conditions either. CI-linked OXPHOS capacity was significantly lower in the ipsilateral hippocampus injected with KA as compared to the respective contralateral hippocampus (Fig. 6B, $p = 0.013$, $F_{3/8} = 4.900$).

*FCR*s of the different substrate and coupling rates are summarized in Fig. 7, using maximum flux (CI&II$_E$) as the reference. Differences were observed for CI$_P$ (Fig. 7B, $p = 0.032$, $F_{3/8} = 3.787$); ipsilateral hippocampus injected with KA differed from contralateral hippocampus of mice injected with KA. The FCR of CII$_E$ revealed an apparent relative upregulation of CII-respiration in the ipsilateral hippocampus injected with KA (Fig. 7D, $p = 0.003$, $F_{3/8} = 7.252$). Apparent ETS excess capacities, $1\text{-}P/E$, (Fig. 7F) did not differ across all conditions.

4. Discussion

The data and data analysis method described above provide deeper understanding of differences in oxidative functions of mitochondria obtained from distinct brain regions. Calculated factors like the apparent excess capacity in conjunction with distinct contributions of specific complexes enable us to hypothesize on the involvement of mitochondria in several neurodegenerative diseases.

A recently published study (Herbst and Holloway, 2015) presented a method to reliably analyze and compare the respiration of different brain regions, while minimizing time and tissue requirements. A fast preparation is crucial to minimize rapidly occurring changes in mitochondrial behavior after dissection. Tissue sample size, oxygen concentrations, temperature and medium-conditions were similar in our method and the one presented by Herbst and Holloway. In contrast, we used catalase containing medium starting from the time point of dissection, in order to preserve the mitochondrial preparations from oxidative modifications. Herbst and Holloway used saponin to permeabilize the brain-samples and report stable respiration of the sample for up to 40 min after tissue preparation. For longer

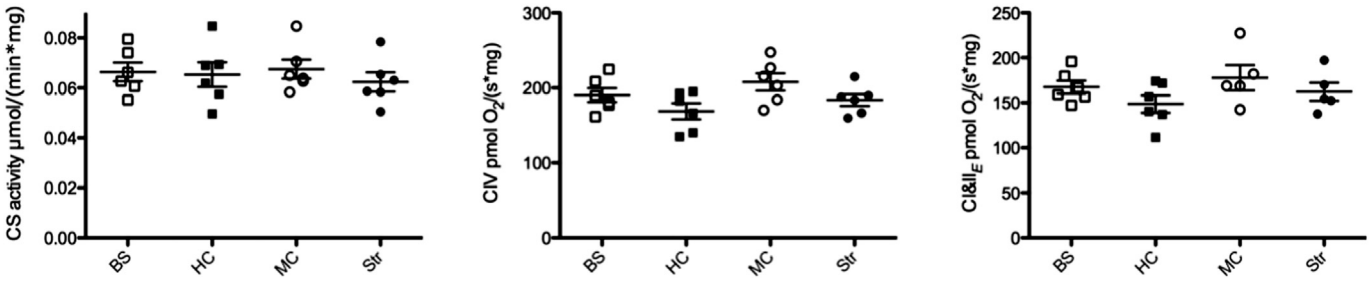

Fig. 1. Citrate synthase (CS), CIV-activity and CI&CII-linked ETS-capacity (CI&CII$_E$ from left to right) were analyzed as functional mitochondrial markers. No differences across brain regions were found for either marker. Electron transfer system (ETS), brainstem (BS), hippocampus (HC), motor cortex (MC), striatum (Str).

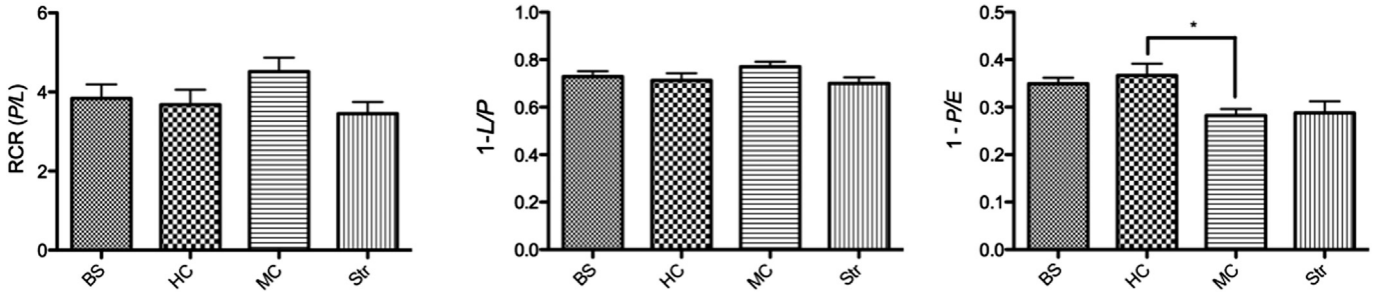

Fig. 2. Respiratory acceptor control ratio (RCR, P/L, left panel) and alternative representation of the RCR as flux control factor (1-L/P, middle panel) revealed no differences between distinct regions of the brain. Biochemical coupling efficiency can therefore be assumed similar. The apparent excess capacity of CI&II-linked ETS over CI&II-linked OXPHOS-capacity (1-P/E, right panel) is higher in HC than in MC. Respiratory limitation by the phosphorylation system is highest in HC. Electron transfer system (ETS), brainstem (BS), hippocampus (HC), motor cortex (MC), striatum (Str). * = $p < 0.05$ one way ANOVA with Tukey's post hoc test.

analyses, chemical permeabilization appears suboptimal, thus we optimized a mechanical permeabilization method. Taken together, these modifications allowed us to measure respiration in a highly reproducible manner, and in longer respirometry protocols than the aforementioned allows. Despite these methodological differences, measured CI linked respiration, which was assessed by similar protocols for naïve cortex was very comparable.

Complementary to Herbst and Holloway's findings, we provide several additional analyses, such as flux control ratios and flux control factors (see Materials and methods section), which allow in-depth characterization of even more mitochondrial parameters.

Assessment of mitochondrial density and normalization of respiration to mitochondrial markers represent a major challenge in functional OXPHOS analysis but are especially important when comparing conditions with expected differences in cell numbers as in models of neurodegenerative diseases. The highly dynamic nature of mitochondria confounds accurate assessment of mitochondrial numbers. Tissue-mass specific respiration integrates the effects of mitochondrial density and activity per unit mitochondrion. Reliable mitochondrial markers are required to separate these component effects. Citrate synthase activity is a commonly used functional marker for the content of intact mitochondria (Holloszy et al., 1970), representing a single-enzyme marker of the mitochondrial matrix. In contrast to CS activity which is determined in an assay separate from the respirometric run ('external' assay), we measured cytochrome *c* oxidase (CIV) activity as an 'internal' step in the respirometric SUIT protocol. Normalization by internal markers yield flux control factors or flux control ratios, which are methodologically independent.

Whereas CIV-activity is also a single-enzyme marker, comparatively independent of further factors, CI&II-linked ETS-capacity comprises the integrated capacity of many parameters influencing respirometry driven by exogenously added substrates for CI and CII. When comparing the three functional mitochondrial markers, we found that all of them give comparable information on mitochondrial density. We therefore conclude that all of them are of equivalent validity in adult, healthy, male mouse brain. Especially when investigating models of brain pathologies, it still is important to evaluate different functional mitochondrial markers due to potential effects of the pathology on distinct enzyme-activities.

In our studies, the results were very similar, when normalized either to CI&II-linked ETS-capacity (Fig. 4) or to citrate synthase activity (Suppl. Fig. 4).

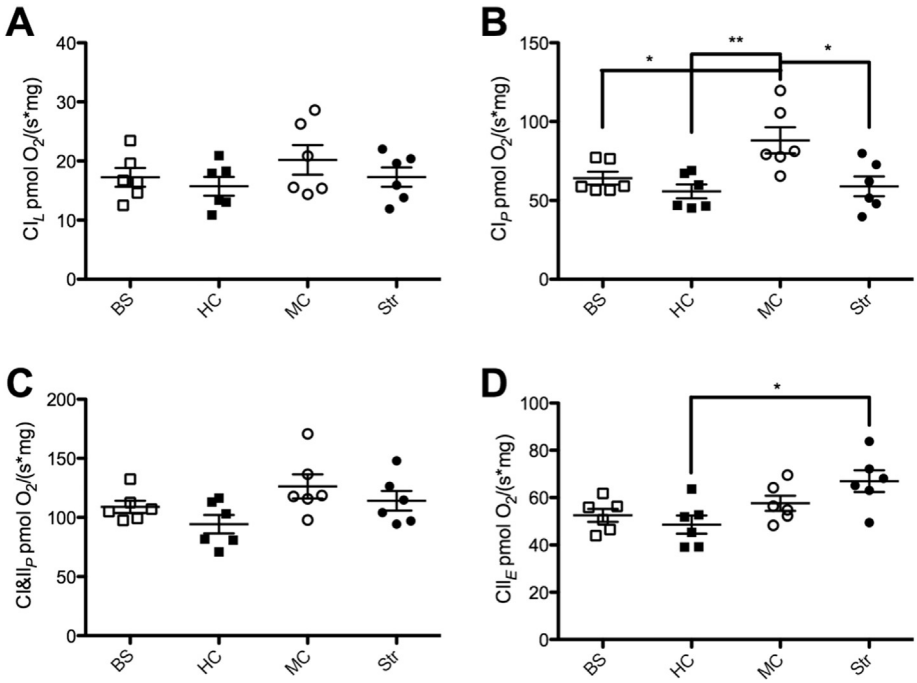

Fig. 3. Tissue mass specific O_2 fluxes in different brain regions are depicted at different stages of the protocol. CI-linked LEAK state after addition of CI substrate, but without ADP (CI_L; A), CI-linked (CI_P; B) and CI&II-linked ($CI\&II_P$; C) OXPHOS-capacity and CII-linked ETS-capacity after addition of the uncoupler (CII_E; D) are shown. Brainstem (BS), hippocampus (HC), motor cortex (MC), striatum (Str). * = $p < 0.05$; ** = $p < 0.01$ one way ANOVA with Tukey's post hoc test.

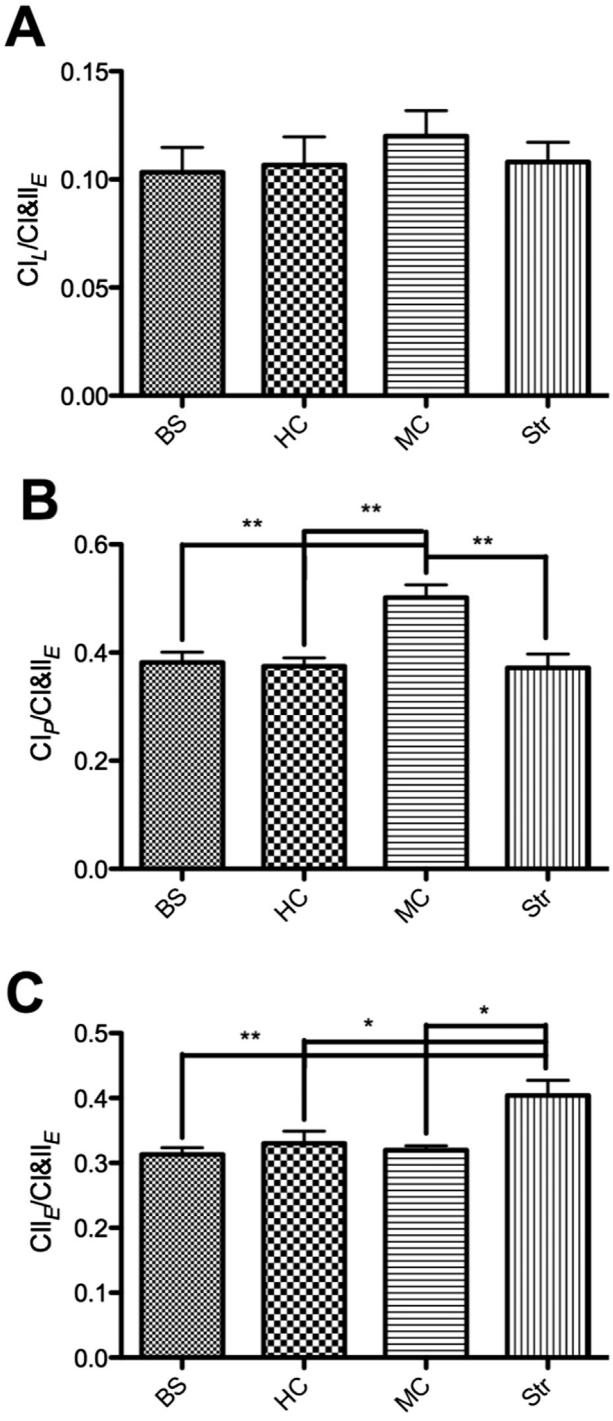

Fig. 4. O_2 fluxes of different brain regions normalized to functional mitochondrial marker CI&CII-linked ETS-capacity (flux control ratios). CI-linked LEAK state (A), CI-linked OXPHOS-capacity (B) and CII-linked ETS-capacity (C) are depicted. Brainstem (BS), hippocampus (HC), motor cortex (MC), striatum (Str). * = $p < 0.05$; ** = $p < 0.01$ one way ANOVA with Tukey's post hoc test.

Our data reveal distinct functional properties of mitochondria in four brain regions, striatum, motor cortex, pons and hippocampus. The brain regions were selected due to their implications in neurodegenerative diseases. For example, striatum is the main area affected in Huntington's disease, cortex and hippocampus are strongly affected in Alzheimer's disease, which may spread starting in brain stem nuclei, and hippocampus is heavily affected in temporal lobe epilepsy.

Coupling/substrate control diagrams (Suppl. Fig. 5) summarize the prominent roles of CI in motor cortex and the importance of CII in striatum. The low apparent excess capacity of CI&II-linked ETS over CI&II-linked OXPHOS in motor cortex and striatum is visible in these diagrams as well (P/E-ratios). These observations may contribute to our understanding of distinct neuronal loss under pathological conditions. For example, in Huntington's disease the mutated huntingtin (mHtt) protein has been shown to impair CII function (Damiano et al., 2013) and neuronal loss in Huntington's disease strongly affects the striatum (Vonsattel and DiFiglia, 1998). mHtt is deleterious to many neuronal subtypes, but medium spiny neurons (MSN) of the striatum are especially vulnerable. Several explanations have been put forth (for review see (Labbadia and Morimoto, 2013), but conclusive explanations of the selective vulnerability of the striatum in Huntington's disease remain elusive. The importance of CII for mitochondrial respiration in the striatum and its inhibition by mHtt in conjunction with lower apparent excess capacity may represent one crucial factor of slowly progressing neuronal loss in this disease.

Considering the proposed importance of mitochondrial dysfunction in numerous neurodegenerative diseases, precise measurement of the distinct contributions of respirational complexes to maximum respirational capacities in different brain regions might contribute to understanding selective vulnerabilities in neuropathological conditions. Therefore, we investigated a model of fast, severe, yet well reproducible neuronal loss - unilateral injection of kainic acid into the dorsal hippocampus.

Unilateral injection of 1 nmol KA into the stratum radiatum of CA1 of mice triggers status epilepticus and epileptogenesis. These processes are accompanied by electro-clinical, behavioral and metabolic alterations (Bouilleret et al., 1999) and cause severe neuronal loss, astrogliosis, granular cell dispersion and mossy fibre sprouting (Suzuki et al., 1995; Bouilleret et al., 1999; Loacker et al., 2007) in a well reproducible manner. Mitochondrial dysfunction seems to be a hallmark in temporal lobe epilepsy (for reviews see (Kudin et al., 2009; Rowley and Patel, 2013). There is mounting evidence for a functional implication of oxidative stress in seizure-induced neuronal damage and loss (for reviews see (Waldbaum and Patel, 2010b). Epilepsy is a common feature of many primary mitochondrial diseases, while the majority of focal epilepsies, such as temporal lobe epilepsy, are induced by traumatic insults (Christensen, 2012). There are a number of studies demonstrating single aspects of mitochondrial functions after acute seizures, like impaired Ca^{2+} sequestering or excessive ROS production (for reviews see (Waldbaum and Patel, 2010b). Also morphological alterations of mitochondria were observed in the hippocampus of epileptic rats (Chuang et al., 2004), ultrastructural abnormalities as well as reduced CI activity have been described in temporal lobe epilepsy in human patients (Kunz et al., 2000) and decreased CI activity has been linked to posttranslational carbonylation of CI during epileptogenesis (Ryan et al., 2012).

Enzyme assays revealed significant depression of the activity of nicotinamide adenine dinucleotide cytochrome c reductase (marker for Complexes I and III) in the KA model in the rat (Chuang et al., 2004). However, studies on multiple components of intact mitochondria are lacking, most probably due to the lack of suitable methods. The contribution and causality of oxidative stress and mitochondrial dysfunction in the process of epileptogenesis and chronic epilepsy are even less well investigated. Our novel protocol enables us to investigate mitochondrial functions from a single dorsal mouse hippocampus in duplicates. Our results show distinct effects ipsi- and contralateral to a unilateral kainic acid injection. These alterations reflect both, alterations in mitochondrial density and differential involvement of distinct mitochondrial complexes.

Qualitative changes in patterns of OXPHOS can be derived from FCRs giving information on changed regulation of OXPHOS, independent from mitochondrial density. We consider this information even more important than the absolute values due to potential inaccuracies in fresh weight measurements and especially in models of cell loss. The FCR of CI_P is lower in KA-injected ipsilateral hippocampi as compared

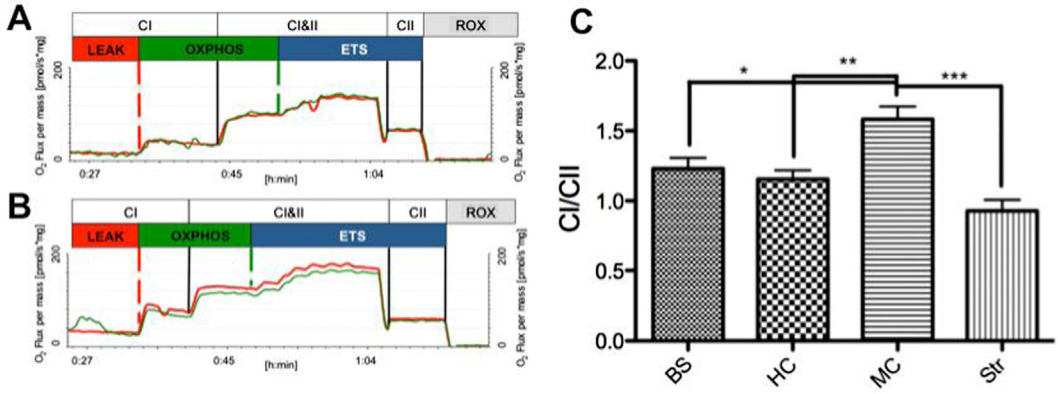

Fig. 5. Respirometric traces of duplicate measurements of striatal (A) and motorcortical (B) tissues are depicted in the left panel. The ratio of CI-linked OXPHOS-capacity and CII-linked ETS-capacity is depicted in the right panel (C), revealing marked differences between distinct regions of the brain. Brainstem (BS), hippocampus (HC), motor cortex (MC), striatum (Str). * = $p < 0.05$; *** = $p < 0.001$ one way ANOVA with Tukey's post hoc test.

to the respective contralateral hippocampi. This seems to be due to decreased respiration in the ipsilateral, but also due to increased respiration contralaterally, which might be due to compensatory mechanisms. Importantly, CII-linked respiration appears to be upregulated only in KA-injected tissue, thereby contributing to similar FCRs of CI&II-linked OXPHOS-capacity across all conditions. An upregulation

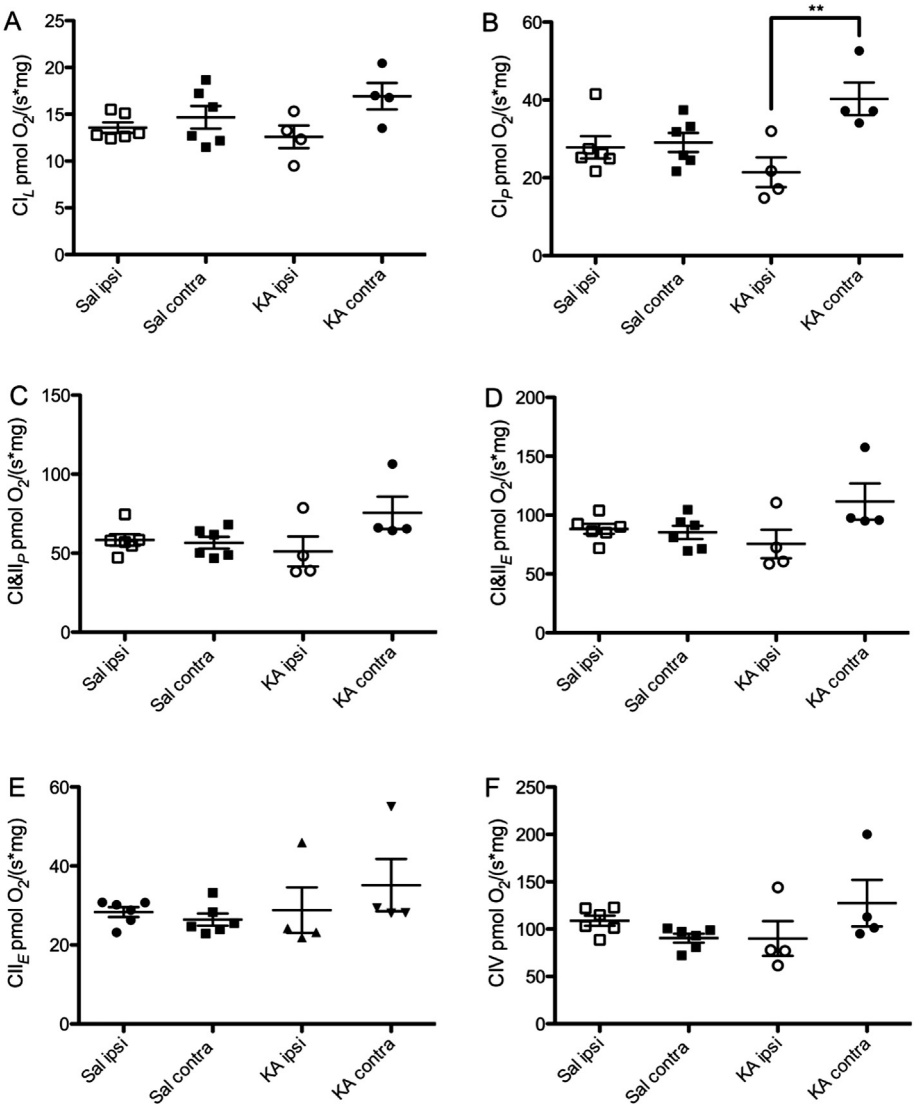

Fig. 6. Tissue mass specific O_2 fluxes are depicted at CI-linked LEAK state (A), CI-linked (B) and CI&II-linked (C) OXPHOS-capacity, CI&II-linked (D) and CII-linked ETS-capacity (E) and for CIV-activity (F). Fluxes of ipsilateral (ipsi) and contralateral (contra) hippocampi of saline (Sal) injected and kainic acid (KA) injected mice are depicted. Dorsal hippocampi were measured in duplicate. ** = $p < 0.01$; one way ANOVA with Tukey's post hoc test.

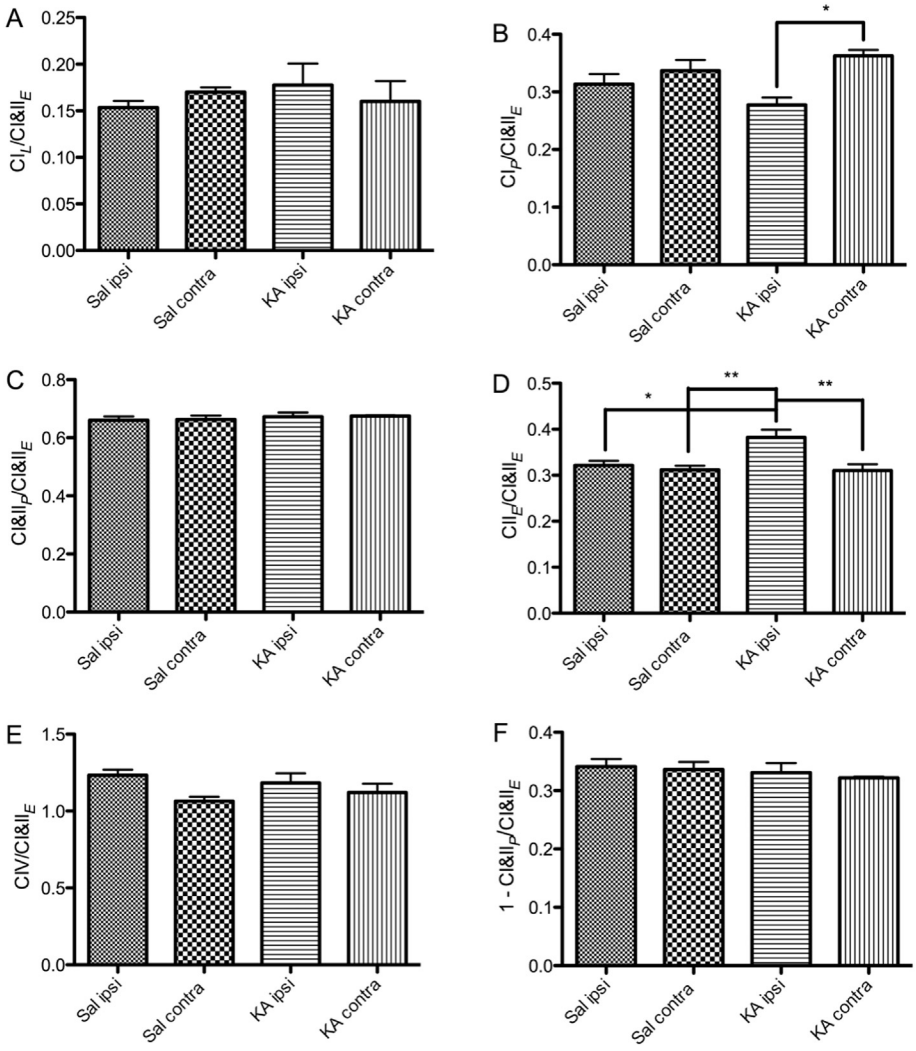

Fig. 7. Flux control ratios in ipsi- and contralateral hippocampal tissues of saline (Sal) and kainic acid (KA) injected mice at CI-linked LEAK state (A), CI-linked (B) and CI&II-linked (C) OXPHOS-capacity, CII-linked ETS-capacity (D) and CIV-activity (E) reveal alterations in the activity of distinct complexes, independent of functional mitochondrial density in the ipsilateral hippocampus. Respiratory limitation by the phosphorylation system is not affected by KA-treatment (F). The apparent excess capacity of CI&II-linked ETS over CI&II-linked OXPHOS-capacity [1-P/E] is similar in all conditions. * = $p < 0.05$; ** = $p < 0.01$ one way ANOVA with Tukey's post hoc test.

of hippocampal CII histological staining in pyramidal cells at a decreased enzyme-activity of CI have already been described in the pilocarpine-induced epilepsy model in rats (Kudin et al., 2002). This report strengthens the validity of our findings as a general mechanism in rodent models of mesial temporal lobe epilepsy.

Thus, the presented kainic-acid experiment demonstrates sensitivity and validity of our method in the study of neurodegenerative diseases. There are, however, several limitations of this experiment regarding OXPHOS in mesial temporal lobe epilepsy mouse models: in particular, we used low sample numbers for this proof-of-priniciple study and investigated only one time point. In order to obtain conclusive information on the involvement of mitochondrial alterations, other time points of epileptogenesis and chronic epilepsy need to be investigated. However, this is beyond the scope of this study.

A strong advantage of the method presented, in comparison to single enzyme assays of complex activities, is its capacity to reveal even subtle shifts in OXPHOS-regulation and to provide a way to assess functional mitochondrial density during respirometry. Therefore, it is possible to attribute observed changes to absolute changes of all functional mitochondrial units or to qualitative changes occurring per mitochondrial unit (FCR). The described apparently compensatory upregulation of CII respiration in epileptic tissue at decreased CI capacity is one such mechanism that is difficult to detect with conventional methods.

In conclusion, the presented method was shown to be sensitive and reliable enough to extract information on several OXPHOS parameters from small brain tissue samples, even if small numbers of experimental animals are used. Moreover, this method enables us to resolve differences in OXPHOS-regulation between brain regions or in distinct disease states in so far unreached detail. The obtained data can be used to calculate indicators for qualitative changes per mitochondrial marker unit (e.g. flux control ratios and flux control factors), for mitochondrial quality control (e.g. respiratory acceptor control ratio) and for potential vulnerability factors (e.g. the apparent excess capacity of the ETS over the phosphorylation system).

Conflict of interest

Erich Gnaiger is the CEO of OROBOROS INSTRUMENTS.

Acknowledgments

This work was supported by the FWF (W1206-B05 and I-977-B24). The authors want to thank Juliana Heidler for the excellent technical support and Meagan McManus for the valuable discussion and linguistic contributions.

Appendix A. Supplementary data

Supplementary data to this article can be found online at http://dx.doi.org/10.1016/j.mito.2015.10.007.

References

Baron, M., Kudin, A.P., Kunz, W.S., 2007. Mitochondrial dysfunction in neurodegenerative disorders. Biochem. Soc. Trans. 35, 1228–1231.

Bouilleret, V., Ridoux, V., Depaulis, A., Marescaux, C., Nehlig, A., Le Gal La Salle, G., 1999. Recurrent seizures and hippocampal sclerosis following intrahippocampal kainate injection in adult mice: electroencephalography, histopathology and synaptic reorganization similar to mesial temporal lobe epilepsy. Neuroscience 89, 717–729.

Christensen, J., 2012. Traumatic brain injury: Risks of epilepsy and implications for medicolegal assessment. Epilepsia 53 (Suppl. 4), 43–47.

Chuang, Y.C., Chang, A.Y., Lin, J.W., Hsu, S.P., Chan, S.H., 2004. Mitochondrial dysfunction and ultrastructural damage in the hippocampus during kainic acid-induced status epilepticus in the rat. Epilepsia 45, 1202–1209.

Crouch, P.J., Blake, R., Duce, J.A., Ciccotosto, G.D., Li, Q.X., Barnham, K.J., Curtain, C.C., Cherny, R.A., Cappai, R., Dyrks, T., Masters, C.L., Trounce, I.A., 2005. Copper-dependent inhibition of human cytochrome c oxidase by a dimeric conformer of amyloid-beta1-42. J. Neurosci. 25, 672–679.

Damiano, M., Diguet, E., Malgorn, C., D'Aurelio, M., Galvan, L., Petit, F., Benhaim, L., Guillermier, M., Houitte, D., Dufour, N., Hantraye, P., Canals, J.M., Alberch, J., Delzescaux, T., Deglon, N., Beal, M.F., Brouillet, E., 2013. A role of mitochondrial complex ii defects in genetic models of Huntington's disease expressing n-terminal fragments of mutant huntingtin. Hum. Mol. Genet. 22, 3869–3882.

Dubinsky, J.M., 2009. Heterogeneity of nervous system mitochondria: location, location, location! Exp. Neurol. 218, 293–307.

Gnaiger, E., 2001. Bioenergetics at low oxygen: dependence of respiration and phosphorylation on oxygen and adenosine diphosphate supply. Respir. Physiol. 128, 277–297.

Gnaiger, E., 2009. Capacity of oxidative phosphorylation in human skeletal muscle: new perspectives of mitochondrial physiology. Int. J. Biochem. Cell Biol. 41, 1837–1845.

Gnaiger, E., 2014. Mitochondrial pathways and respiratory control. An Introduction in Oxphos Analysis.

Gu, M., Gash, M.T., Mann, V.M., Javoy-Agid, F., Cooper, J.M., Schapira, A.H., 1996. Mitochondrial defect in Huntington's disease caudate nucleus. Ann. Neurol. 39, 385–389.

Herbst, E.A., Holloway, G.P., 2015. Permeabilization of brain tissue in situ enables multiregion analysis of mitochondrial function in a single mouse brain. J. Physiol. 593, 787–801.

Hirsch, E., Graybiel, A.M., Agid, Y.A., 1988. Melanized dopaminergic neurons are differentially susceptible to degeneration in Parkinson's disease. Nature 334, 345–348.

Holloszy, J.O., Oscai, L.B., Don, I.J., Mole, P.A., 1970. Mitochondrial citric acid cycle and related enzymes: adaptive response to exercise. Biochem. Biophys. Res. Commun. 40, 1368–1373.

Kudin, A.P., Kudina, T.A., Seyfried, J., Vielhaber, S., Beck, H., Elger, C.E., Kunz, W.S., 2002. Seizure-dependent modulation of mitochondrial oxidative phosphorylation in rat hippocampus. Eur. J. Neurosci. 15, 1105–1114.

Kudin, A.P., Zsurka, G., Elger, C.E., Kunz, W.S., 2009. Mitochondrial involvement in temporal lobe epilepsy. Exp. Neurol. 218, 326–332.

Kunz, W.S., Kudin, A.P., Vielhaber, S., Blumcke, I., Zuschratter, W., Schramm, J., Beck, H., Elger, C.E., 2000. Mitochondrial complex I deficiency in the epileptic focus of patients with temporal lobe epilepsy. Ann. Neurol. 48, 766–773.

Labbadia, J., Morimoto, R.I., 2013. Huntington's disease: underlying molecular mechanisms and emerging concepts. Trends Biochem. Sci. 38, 378–385.

Lange, H., Thorner, G., Hopf, A., Schroder, K.F., 1976. Morphometric studies of the neuropathological changes in choreatic diseases. J. Neurol. Sci. 28, 401–425.

Loacker, S., Sayyah, M., Wittmann, W., Herzog, H., Schwarzer, C., 2007. Endogenous dynorphin in epileptogenesis and epilepsy: anticonvulsant net effect via kappa opioid receptors. Brain 130, 1017–1028.

Perry, C.G., Kane, D.A., Lanza, I.R., Neufer, P.D., 2013. Methods for assessing mitochondrial function in diabetes. Diabetes 62, 1041–1053.

Pesta, D., Gnaiger, E., 2012. High-resolution respirometry: oxphos protocols for human cells and permeabilized fibers from small biopsies of human muscle. Methods Mol. Biol. 810, 25–58.

Renner, K., Kofler, R., Gnaiger, E., 2002. Mitochondrial function in glucocorticoid triggered t-all cells with transgenic bcl-2 expression. Mol. Biol. Rep. 29, 97–101.

Rowley, S., Patel, M., 2013. Mitochondrial involvement and oxidative stress in temporal lobe epilepsy. Free Radic. Biol. Med. 62, 121–131.

Ryan, K., Backos, D.S., Reigan, P., Patel, M., 2012. Post-translational oxidative modification and inactivation of mitochondrial complex I in epileptogenesis. J. Neurosci. 32, 11250–11258.

Schapira, A.H., Cooper, J.M., Dexter, D., Jenner, P., Clark, J.B., Marsden, C.D., 1989. Mitochondrial complex I deficiency in Parkinson's diseaseParkinson's disease. Lancet 1, 1269.

Suzuki, F., Junier, M.P., Guilhem, D., Sorensen, J.C., Onteniente, B., 1995. Morphogenetic effect of kainate on adult hippocampal neurons associated with a prolonged expression of brain-derived neurotrophic factor. Neuroscience 64, 665–674.

Vonsattel, J.P., DiFiglia, M., 1998. Huntington disease. J. Neuropathol. Exp. Neurol. 57, 369–384.

Waldbaum, S., Patel, M., 2010a. Mitochondrial dysfunction and oxidative stress: a contributing link to acquired epilepsy? J. Bioenerg. Biomembr. 42, 449–455.

Waldbaum, S., Patel, M., 2010b. Mitochondria, oxidative stress, and temporal lobe epilepsy. Epilepsy Res. 88, 23–45.